# Zr alloy protection against high-temperature oxidation: Coating by a double-layered structure with active and passive functional properties

Irena Kratochvílová[a,*], Petr Ashcheulov[a], Jan Škarohlíd[b], Radek Škoda[b], Jaromír Kopeček[a], Petr Sajdl[c], Jan Macák[c], Magdaléna Lajčinová[d], Adéla Nováková[d], Johannes Neethling[e], Arno Janse van Vuuren[e], Sinoyolo Ngongo[e], Peng Xu[f], Jan Lorinčík[g], Martin Steinbrück[h]

[a] Institute of Physics of the Czech Academy of Sciences, Na Slovance 2, CZ-182 21, Prague 8, Czech Republic
[b] Czech Technical University in Prague, Czech Institute of Informatics, Robotics and Cybernetics, Jugoslávských partyzánů 1580/3, Prague 6, CZ-160 00, Czech Republic
[c] University of Chemistry and Technology, Power Engineering Department, Technická 3, Prague 6, CZ-166 28, Czech Republic
[d] Faculty of Nuclear Physics and Physical Engineering, Czech Technical University in Prague, Zikova 1, 160 00, Prague 6, Czech Republic
[e] Centre for HRTEM, Department of Physics, Nelson Mandela University, Port Elizabeth, South Africa
[f] Nuclear Fuel Division, Westinghouse Electric Company, 5801 Bluff Road, Hopkins, SC, 29209, USA
[g] Research Centre Řež, Hlavní 130, CZ-250 68, Husinec-Řež, Czech Republic
[h] Institute for Applied Materials (IAM), Karlsruhe Institute of Technology, Hermann-von-Helmholtz-Platz 1, 76344, Eggenstein-Leopoldshafen, Germany

ARTICLE INFO

*Keywords:*
High temperature corrosion
Zr nuclear tubes
Double layer protective coating
Nanocrystalline diamond coating
CrAlSiN

ABSTRACT

In this work, a new concept of metal surface protection against degradation caused by high-temperature oxidation in water environment is presented. We were the first to create a double-layered coating consisting of an active and passive part to protect Zr alloy surface against high-temperature oxidation in a hot water environment. We investigated the hot steam corrosion of ZIRLO fuel cladding coated with a double layer consisting of 500 nm nanocrystalline diamond (NCD) as the bottom layer and 2 μm chromium-aluminum-silicon nitride (CrAlSiN) as the upper layer. Coated and uncoated ZIRLO samples were exposed for 4 days at 400 °C in an autoclave and for 60 min at 1000 °C (nuclear reactor accident temperature) in a hot steam furnace. We have shown that the NCD coating protects the Zr alloy surface against oxidation in an active way: carbon from NCD layer enters the Zr alloy surface and, by changing the physical and chemical properties of the Zr cladding tube surface, limits the Zr oxidation process. In contrast, the passive CrAlSiN coating prevents the Zr cladding tube surface from coming into physical contact with the hot steam. The advantages of the double layer were demonstrated, particularly in terms of hot (accident-temperature) oxidation kinetics: in the initial stage, CrAlSiN layer with low number of defects acts as an impermeable barrier. But after a longer time (more than 20 min) the protection by more cracked CrAlSiN decreases. At the same time, the carbon from NCD strongly penetrates the Zr cladding surface and worsen conditions for Zr oxidation. For the double-layer coating, the underlying NCD layer mitigates thermal expansion, reducing cracks and defects in upper layer CrAlSiN.

## 1. Introduction

Zirconium alloys are used in light water and heavy water nuclear reactors. Zirconium alloys have low parasitic absorption of neutrons, high resistance against radiation damage and appropriate mechanical properties. In nuclear reactor Zr alloy interacts with hot water or steam. In this case, water molecules are dissociated and both oxygen and hydrogen ions penetrate into the Zr alloy which is then less dense more fragile [1 5]. It was also shown that high temperature oxidation of zirconium alloys is accompanied by stresses in the oxide parts. These stresses may reflect on the protective properties of the oxide scale, which results in reducing the life time of the substrate by e.g. cracking of the oxide layer, accelerating the oxidation process [1 5].

Protection of nuclear fuel claddings against high temperature oxidation and hydrogenation in water cooled nuclear reactors is crucial step towards nuclear safety and operability [6 11]. One of the safety criteria for fuel rod operation in commercial reactors is the restriction of oxide film thickness [12 14]. Even if different Zr alloys such as ZIRLO (USA) M5 (France) and E series (Russia) have been developed to have high corrosion resistance, the problems of high temperature oxidation and hydrogenation of Zr alloy fuel claddings still remain [8,15 25]. So, the proper protection of zirconium fuel rod surfaces

* Corresponding author.
*E-mail address:* krat@fzu.cz (I. Kratochvílová).

against oxidation in nuclear reactor environments can extend the life time of the nuclear fuel and enhance operation safety at accident temperatures [26].

A common strategy for the protection of metal surfaces against high temperature oxidation in a water environment is to separate the metal surface from the surrounding hot water/steam by a water impermeable coating [14] on the order of tens of μm thick or by a coating that forms oxides with very low oxidation kinetics. A complication in this type of surface protection is that each defect, pore or crack in the coating causes oxidation to develop, so places under these defects are more oxidized than uncoated nuclear fuel tubes treated under the same conditions. This situation is a typical consequence of the oxidation process and changes in substrate temperature and volume.

We designed and tested a double layered structure consisting of a water permeable (bottom, active) and water impermeable (top, pas sive) layer. To prove a new concept for protecting metal surface against oxidation in hot water environment by using a double layer coating we coated Zr alloy (ZIRLO) nuclear fuel claddings by 500 nm active na nocrystalline diamond (NCD) [27,28] as the bottom layer and 2 μm passive chromium aluminum silicon nitride (CrAlSiN) alloy as the upper layer [9,27 31]. Water permeable and soft NCD layer was de posited on the surface of ZIRLO cladding by a microwave plasma en hanced linear antenna chemical vapor deposition (MW LA PECVD) device [32,33]. An impermeable chromium aluminum silicon nitride (CrAlSiN) [34] coating was deposited using the standard commercially available method of physical vapor deposition.

In our work coated and uncoated ZIRLO samples were exposed to 400 °C in autoclave for 4 days and nuclear reactor accident tempera tures (1000 °C in steam furnace) for 60 min [30,31]. For samples ex posed to 1000 °C, hot steam oxidation kinetics were also measured. The bottom part of the double layered coating was water permeable NCD. The NCD layer consisted of two different carbon phases: $sp^3$ hybridized carbon/diamond and $sp^2$ hybridized carbon [32]. As shown in our previous works [27,28,30], the protective NCD layer reduces Zr nuclear fuel cladding oxidation at operating temperatures (by 30 50%), which prolongs the lifetime of the nuclear cladding and consequently en hances nuclear fuel burn up [30,31,35]. Specifically, when standard ASTM procedure [36] was applied (195 days, 360 °C hot water) oxi dation of NCD coated samples decreased significantly (50%). The average hydrogen concentration is markedly greater for uncoated samples than NCD coated samples [27]. After ion beam irradiation (10 dpa, 3 MeV $Fe^{2+}$), a diamond layer showed structural integrity, with both $sp^3$ and $sp^2$ carbon phases [13].

NCD coating worked as a bottom part in a double layer coating because of complex and specific way how NCD coating protects Zr alloy against corrosion [27]. In [27] we have showed that NCD main function as corrosion protective coating is based on the fact that small amount of carbon atoms diffused during autoclave/hot steam treatment from NCD into $ZrO_2$ surface layer which change $ZrO_2$ electrical properties (semi conductivity). Amount of carbon diffused from NCD coating corre sponds to density of doping in extrinsic semiconductor $10^{16}$at/cm$^3$ (amount of carbon atoms in NCD layer is in order $10^{23}$ at/cm$^3$) which does not significantly influence ZIRLO tube mechanical properties but worsen conditions for Zr oxidation process at $Zr/ZrO_2$ interface in nu clear reactor environment [27]. As was shown [27] NCD coated ZIRLO tube samples both autoclaved 4 days at 400 °C and treated 195 days in hot water (360 °C, ASTM standard procedures) had NCD layer con taining standard full diamond phase. We have also patented a poly crystalline diamond layer as a protective coating for Zr alloys used in nuclear reactors [37].

We were the first who showed the protection ability and oxidation kinetics of NCD (active) and CrAlSiN (passive) double layer coating on ZIRLO nuclear fuel cladding at working and accident water cooled nuclear reactor temperatures. For all tested samples, the relative weight gain after hot steam oxidation was determined. According to [14], these weight gains are caused mainly by oxidation and hydrogen uptake by the autoclaved ZIRLO samples. Several types of further measurements were performed to analyze the effect of high temperature oxidation on coated Zr nuclear fuel tubes: mass online thermogravimetry (mea surement of the mass changes caused by oxidation), optical microscopy of metallographic cross sections of samples, X ray photoelectron spec troscopy (XPS), Raman spectroscopy, electron microscopy (transmis sion electron microscopy (TEM) and scanning electron microscopy (SEM)), secondary ion mass spectrometry (SIMS) and electrochemical impedance measurements, which proofed to be efficient tool to study high temperature corrosion of structural materials for nuclear industry in both in situ [38,39] and ex situ application, as e.g. was the case of NCD coated ZIRLO. While in the former application instant corrosion rate can be determined, in the letter one electronic and other properties of the corrosion product films can be tested. In this work impedance measurements were used to assess electronic properties of oxide layer formed on ZIRLO during exposure at 400 °C and to estimate thickness of surface layers after exposure of ZIRLO samples at 1000 °C.

## 2. Materials and methods

### 2.1. NCD coating

ZIRLO (Sn 1 0,7%; Fe 0,1%; O 0,13%; Nb 1%) fuel cladding 25 mm cuts were put in a seeding (colloidal solution of diamond nano particles). For ZIRLO samples NCD coating we used MW LA PECVD apparatus in the Institute of Physics AS CR, Na Slovance 2, Prague 8, Czech Republic, constructed by Michael Lear. We applied gasses $H_2$ + $CH_4$ + $CO_2$, pressure less than 1 mbar, a microwave power of 2 × 3 kW, temperature 600 °C. Due to diffuse plasma at low pressures, the NCD coating was over the outer circumference of ZIRLO tubes put horizontally in the deposition chamber. The thickness of the NCD layer coating on the ZIRLO tubes was 500 nm.

### 2.2. CrAlSiN coating

CrAlSiN was deposited on ZIRLO nuclear fuel rod samples using the standard commercially available method of physical vapor deposition (PVD). The composition of nitrides in the coating was 36.5% Al, 4.8% Si, and 58.7 Cr. To determine the impact of CrAlSiN cracking, the thickness of the coating was 2 μm. Samples were coated only on the outer surface. The maximal solubility of aluminum in the Cr1 − xAlxN structure is usually limited to 0.6 0.8 before wurtzite type aluminum nitride is formed. Alloying the CrAlN structure with silicon significantly affects the grain size and mechanical properties. In this quaternary CrAlSiN structure, silicon tends to segregate as amorphous SixNy along the grain boundaries. This effect leads to a nanocomposite structure with improved oxidation resistance. The oxidation resistance of CrAlSiN coatings has been found to be excellent, typically out performing that of CrAlN.

### 2.3. Simulation of standard and accident hot steam conditions in a nuclear reactor

To simulate the ability of NCD coating to protect ZIRLO cladding against oxidation at standard and accident specific hot steam condi tions in a nuclear reactor, NCD coated ZIRLO fuel cladding, CrAlSiN coated ZIRLO fuel cladding, NCD and CrAlSiN coated ZIRLO fuel cladding, and reference uncoated ZIRLO fuel cladding samples were subjected to 400 °C autoclave (400 °C/4 days at 15 MPa) and 1000 °C hot steam tests. The oxidation kinetics of the samples were measured in a Netzsch STA449 F3 Jupiter with a steam furnace coupled with an Aeolos mass spectrometer. Samples were treated for 1 h at 1000 °C; heating was performed in Ar at 20 K/min, and cooldown was performed in Ar at 50 K/min. The atmosphere during the oxidation phase was 2 g/h $H_2O$ + 50 ml/min Ar (protective gas), corresponding to $PH_2O$ = 0.45 bar. The pressure in the chamber is round 1 bar.

Reference tests with inert alumina tube segments of similar size resulted in mass changes during the steam isothermal phase of less than 100 µg. Samples were placed in a platinum mesh sample holder to ensure si milar flow conditions in and outside the tube segment samples with a distance ring made of alumina to avoid interactions between Zr and Pt.

### 2.4. Optical and electron microscopies

Metallographic cross sections of samples for optical microscopy were prepared from cuts of ZIRLO nuclear fuel rods and imaged by utilizing an optical magnifying instrument. The cuts of the samples were hot squeezed into a appropriate material for test examinations through optical microscopy. NCD and CrAlSiN coatings were displayed by a Tescan FERA 3 scanning electron microscope. An accelerating voltage of 5 kV was used. Elemental composition analysis was per formed using an EDS EDAX Octane Super 60 $mm^2$ detector with an acceleration voltage of 20 kV. TEM specimens were prepared using a Helios Nanolab 650 focused ion beam (FIB) SEM and investigated in a JEOL 2100 TEM operated at 200 kV.

### 2.5. Secondary ion mass spectrometry

SIMS measurements were performed using a magnetic sector SIMS IMS 7f (Cameca) in 3D profiling mode with the following main in strumental parameters: $Cs^+$ primary ions, 20 nA primary ion current, 15 keV impact energy, raster size 100 µm, mass resolving power 4000, negative secondary ion polarity, pressure in the analytical chamber $1 \times 10^{-9}$ mbar. The 3D mode was chosen to visualize lateral in homogeneity of the SIMS signal, which was expected because of surface roughness and polycrystalline character of the sample. A depth profile from a 50 µm size area placed in the center of the crater area was constructed in the post processing of the 3D SIMS data. We calibrated the depth scale of the profile by profilometer. The calibration of the concentration scale was not attempted since SIMS is not a suitable technique for matrix element quantification.

### 2.6. X ray photoelectron spectroscopy and Raman spectroscopy

The ESCA Probe P type produced by Omicron Nanotechnology was used for all XPS measurements. Monochromatized X ray radiation with energy 1486.7 eV creates photoelectrons which were analyzed in con stant analyzer energy mode with pass energy of 50 eV for overview spectra and 20 eV or 30 eV used for detailed analysis. Electron gun working with very low energies of radiated electrons (approx. from 1 eV up to 2,5 eV) compensate the possible charging of analyzed surfaces. The preparation chamber is connected with ion gun of type ISE5 which was operated at an energy of 5 keV.

Intensity calibration was based on measurements of copper under the same conditions as analyzed samples. Detail characteristics of the XPS machine checked by measurements of silver and carbon lines. CASA XPS software was used to determine the areas of the lines and database of relative sensitivity factors enable to identify elemental concentrations. The XPS databanks help us to define the chemical species.

To find the NCD layer setting ($sp^2$ and $sp^3$ hybridized carbon), the layers were analyzed by Raman spectroscopy [1]. Method was per formed at room temperature utilizing a Renishaw InVia Raman device. Laser excitation wavelength was 488 nm. Spectra were obtained at different points to test the homogeneity of the coating. Raman spectra of samples after autoclave testing were gathered.

### 2.7. Capacitance measurements

To assess charge transfer properties of the samples Mott Schottky plots (capacitance vs. potential dependence) were measured. All mea surements were performed in a standard electrochemical cell at room temperature in 0.5 M $K_2SO_4$ using Reference 600 electrochemical system (Gamry, USA). A 3 electrode setup was used, incorporating the reference electrode (saturated calomel electrode SCE) and the platinum mesh coaxial to the working electrode as counter electrode. As working electrodes served the samples of ZIRLO tubes equipped with a contact and lead in the internal part. The internal part was isolated using sili cone sealant, so only the outer part of the tube surface was exposed during the measurements. About 30 min were usually needed to stabi lize OCP. The capacitance dependence on potential was measured in the potential range of − 1 V to + 1 V vs. OCP at the constant frequency of the perturbation signal of 1 kHz. The polarization voltage was applied in 100 mV steps in the direction from negative to positive potential. At high frequencies double layer effects can be neglected and the potential dependence of space charge capacitance of n type semiconductor can, according to Mott Schottky theory, be expressed as:

$$\frac{1}{C^2} = \frac{2}{\varepsilon_r \varepsilon_0 N_D q}\left(V - V_{fb} - \frac{kT}{q}\right) \quad (1)$$

$\varepsilon_r$ is the surface layer dielectric constant ($\varepsilon_r = 23$ oxide film, and $\varepsilon_r = 10 - 17$ samples coated by NCD) after 400 °C hot steam oxidation, $\varepsilon_0$ is vacuum permittivity, $N_D$ is the density of electron donors in the surface layer ($cm^{-3}$), $q$ is the elementary charge, $V$ and $V_{fb}$ are applied and flat band potentials respectively, $k$ is the Boltzmann constant and $T$ is the absolute temperature

## 3. Results and discussion

### 3.1. Oxidation of autoclaved samples

We compared the protective effect of the 500 nm NCD coating, the 2 µm CrAlSiN coating and the double layer coating consisting of 500 nm NCD as the bottom layer and 2 µm CrAlSiN as the top layer on ZIRLO tubes. Coated and bare ZIRLO fuel cladding tubes were subjected to 400 °C hot steam treatment for 4 days and to 1000 °C hot steam treat ment for 60 min during tests. The presence of protective NCD coating, CrAlSiN coating and double layers coating was confirmed by Raman spectroscopy, SEM imaging, SIMS and optical microscopy, as shown below. For all tested samples, the relative weight gain was calculated from the difference between the sample weight before and after oxi dation including material released from the sample during hot steam/ autoclave treatments. Weight gains of all the samples were normalized to the relevant/coated area of the tube surface: the inner surfaces of the ZIRLO tubes were not fully covered by the NCD and/or CrAlSiN (con firmed by SEM imaging and Raman spectroscopy) as the coating was unable to fully penetrate into a tube's internal structure. We re calculated the weight gain to NCD, CrAlSiN and double layer coated parts of the tubes (covered was full outer surface and 40 60% of the inner surface). From total weight gain of coated and hot steam/auto clave treated samples we subtracted the weight gain which corresponds to the uncovered parts of treated tubes (obtained from uncovered treated tubes weight gain). From these results we calculated weight gain of the coated parts of the samples in $g.m^{-2}$ (Tables 1 and 2). Comparable results have been obtained for autoclaved NCD coated ZIRLO tubes previously [27,28].

After 4 days at 400 °C in a hot steam autoclave, the oxidation of NCD coated ZIRLO tubes was reduced 56% compared to that of un coated ZIRLO tubes treated under the same conditions (Table 1). However, the double layer coated ZIRLO tubes treated for 4 days at 400 °C under hot steam showed very low oxidation a relative weight gain of only 12% compared to that of the uncoated (bare) ZIRLO samples treated under the same conditions (Table 1). The 2 µm CrAlSiN coating had a comparable ability to protect the ZIRLO tube against oxidation under 400 °C hot steam autoclave treatment (4 days) as double layer coating. According to [29,40 43] high protective ability of impermeable CrAlSiN coating and double layer coating means that the

**Table 1**
Weight gains in bare ZIRLO, 500 nm NCD-coated ZIRLO and ZIRLO coated with a double layer of 500 nm NCD and 4 μm CrAlSiN after exposure to 400 °C hot steam oxidation for 4 days. The relative weight gain is calculated for each sample as the % of unprotected ZIRLO weight gain. The lowest weight gain/lowest oxidation was measured for ZIRLO coated with a double layer of 500 nm NCD and 4 μm CrAlSiN. We recalculated (normalized) the weight gain to NCD, CrAlSiN and double layer coated parts of the tubes.

| ZIRLO sample coating | Weight gain [g m $^{2}$] | Relative weight gain (% of ZIRLO wg) |
|---|---|---|
| NCD + CrAlSiN | 0.41 | 12 |
| NCD | 1.894 | 56 |
| CrAlSiN | 0.51 | 15 |
| No coating | 3.36 | 100 |

CrAlSiN coating is not significantly destroyed after 4 days in the autoclave and can act as an impermeable barrier (Fig. S2). This result also confirms good adhesion of CrAlSiN coating to both ZIRLO surface and to NCD coated ZIRLO surface. Future step will be corrosion tests of double layer coated ZIRLO samples processed for longer time in autoclave and processed according to ASTM procedure [36]. The amount of defects/cracking on double coating and 2 μm CrAlSiN coating after 4 days in 400 °C autoclave is small which correlate with the fact that oxidation of both double coated and CrAlSiN coated ZIRLO samples are low and close to each other (Table 2) and which is further confirmed by SEM (see below).

To investigate the oxidation of double layer coated ZIRLO samples under conditions when the CrAlSiN layer is according to [29,44 46] cracked, we tested the critical oxidation kinetics of samples treated for 60 min at accident temperatures under hot steam. The oxidation kinetics of all coated samples autoclaved at 1000 °C showed that the coating materials had different protection mechanisms against oxidation. All data are available from graphs presented in Data in Brief file using standard ORIGIN software.

During initial oxidation in the 1000 °C hot steam autoclave (< 10 min), the oxidation of the ZIRLO tube coated with CrAlSiN and the ZIRLO tube coated with the double layer was lower than that of the uncoated ZIRLO and NCD coated ZIRLO tube [29] at this initial phase, CrAlSiN acted as an effectively impermeable barrier. The corrosion of bare ZIRLO and NCD coated ZIRLO was similar (see Table 2. and Fig. 1) carbon diffusion from NCD coating just begins and does not significantly affect oxidation kinetics of zirconium alloy. On the contrary, CrAlSiN and double layer coating at this initial stage importantly affect the typical oxidation kinetics of zirconium which can be obtained mainly due to small amount of defects in CrAlSiN coating [29,46]. Hydrogen release measurements showed that for less than 5 min in the hot steam furnace, CrAlSiN worked as a barrier, preventing steam access to the Zr alloy surface smallest amount of hydrogen was released from water dissociation on ZIRLO surface for CrAlSiN coated and double layer coated ZIRLO samples. After longer time (7 26 minutes) in 1000 °C hot steam the lowest hydrogen amount from all the tested samples was released in the case of NCD coated ZIRLO tube.

After a longer period in 1000 °C hot steam (> 10 min), the oxidation of 2 μm thick CrAlSiN coated sample was higher than NCD coated and double layer coated samples (Fig. 1). At this stage, carbon from NCD coating more effectively diffuse into growing $ZrO_2$ layer and by changing its electrical properties decrease ZIRLO corrosion [29]. After 30 min in 1000 °C hot steam, NCD coating and double layer coating effectively protected the ZIRLO tube (Table 2, Fig. S1). In this case, the just 2 μm thick CrAlSiN coating protective ability is destroyed CrAlSiN practically did not protect the ZIRLO tube against oxidation (Fig. 1). The normalized weight gain (oxidation) of the NCD and double layer coated ZIRLO samples (1000 °C, 30 min) decreased by 16 and 17%, respectively compared to uncoated ZIRLO oxidation (Table 2., Fig. S1). NCD layer as prepared is 0.5 μm thick, CrAlSiN layer as prepared is 2 μm thick, $ZrO_2$ layer on uncoated ZIRLO surface after 60 min 1000 °C hot steam is round 200 mm thick [27,28] which was confirmed by optical microscopy results (see below). It should be noted that the normalized weight added by the NCD coating represents less than 2% or 1.4% of the normalized weight gain for the ZIRLO tubes after 1000 °C hot steam, 30 or 60 min respectively. NCD coated ZIRLO tube normalized weight gain decreased after 1000 °C hot steam treatment by 16% (30 min) and 13% (60 min) compared to normalized weight gain of uncoated ZIRLO samples after same treatment.

The oxidation of ZIRLO coated with CrAlSiN after 1 h at 1000 °C under hot steam was essentially the same as that of uncoated ZIRLO treated under the same conditions. The oxidation of ZIRLO tubes coated with NCD and ZIRLO tubes coated with the double layers after 1 h at 1000 °C was 13% (NCD) and 8% (double layer) lower than that of bare ZIRLO tube treated under the same conditions. State of samples after 60 min 1000 °C in hot steam was investigated by SIMS, XPS, optical microscope and SEM. Measured oxidation of coated and uncoated samples treated 60 min 1000 °C in hot steam correspond to results obtained from SEM and optical microscopy see below (Figs. 2 6, S3). In all cases for coated ZIRLO samples the outer $ZrO_2$ layer thickness is lower than uncoated inner ZIRLO sample surface. Ratio of thickness of $ZrO_2$ layer under the CrAlSiN coated surface related to $ZrO_2$ thickness of uncoated (inner) part of the same sample was biggest compared to $ZrO_2$ layer in NCD and double layer coated ZIRO.

The kinetics of hydrogen release of the ZIRLO tube surface in the 1000 °C hot steam furnace are presented in Fig. 1b. Hydrogen release measurements confirmed that for short times in the hot steam furnace (less than 5 min), CrAlSiN worked as a barrier, preventing steam access to the Zr alloy surface less amount of hydrogen was after such a short time released from water dissociation on ZIRLO surface for CrAlSiN coated and double layer coated ZIRLO samples. After longer time (7 26 minutes) in 1000 °C hot steam the lowest hydrogen amount from all the tested samples was released in the case of NCD coated ZIRLO tube.

Importantly, from our results we can deduce that the double layer coating combined both advantages at accident temperature in the hot steam furnace: at the initial autoclave stage, CrAlSiN acted as a barrier against water molecules/oxidation, and after 10 min in the1000 °C hot steam, the water permeable NCD coating more effectively worsened the conditions for Zr oxidation. As substrate and coating materials (ZIRLO, CrAlSiN) have different thermo mechanical properties, stress develops mainly in the high temperature processed coated samples [47]. This

**Table 2**
Weight gains of bare ZIRLO, 500 nm NCD-coated ZIRLO and ZIRLO coated with a double layer of 500 nm NCD and 4 μm CrAlSiN after exposure to 1000 °C hot steam oxidation for 10 and 30 min. The relative weight gain is calculated for each sample as the % of uncoated ZIRLO weight gain. We recalculated (normalized) the weight gain to NCD, CrAlSiN and double layer coated parts of the tubes.

| ZIRLO sample coating | Relative weight gain (% of ZIRLO wg) after 10 minutes in 1000 °C autoclave | Relative weight gain (% of ZIRLO wg) after 30 minutes in 1000 °C autoclave |
|---|---|---|
| NCD + CrAlSiN | 28 | 83 |
| NCD | 99 | 84 |
| CrAlSiN | 42 | 97 |
| No coating | 100 | 100 |

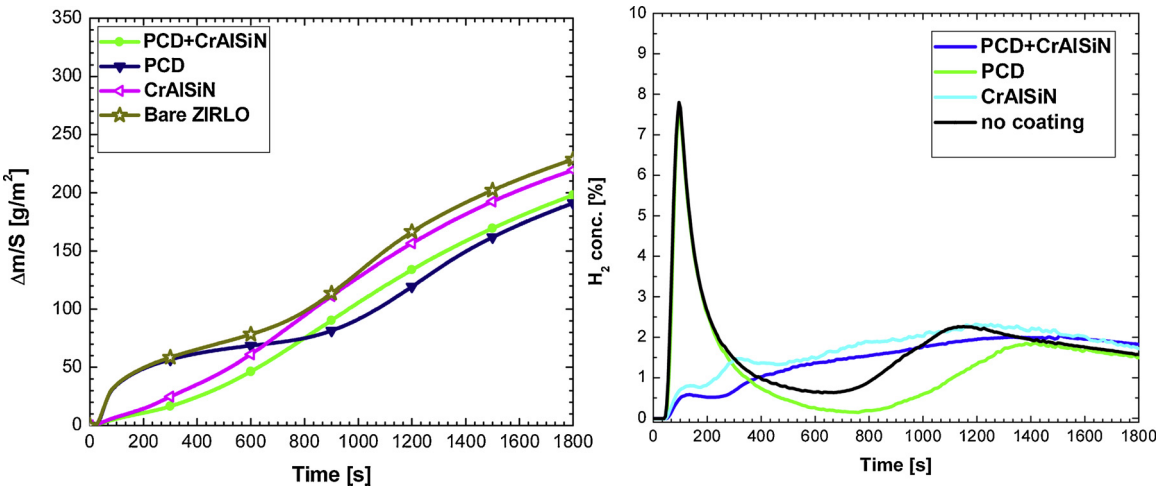


**Fig. 1.** a) The oxidation kinetics of samples oxidized at 1000 °C under hot steam showed that the coating materials had different methods of protection against oxidation. For short times in the hot steam furnace (less than 10 min), 2 μm CrAlSiN worked as barrier against oxidation – CrAlSiN coating protected ZIRLO tube more than permeable NCD coating. For longer times in the autoclave (more than 10 min), the oxidation of the CrAlSiN layer-coated Zr tube was higher than that of the double layer- and NCD-coated ZIRLO tubes. b) Hydrogen release measurements showed that for less than 5 min in the hot steam furnace, CrAlSiN worked as a barrier, preventing steam access to the Zr alloy surface – smallest amount of hydrogen was released from water dissociation on ZIRLO surface for CrAlSiN coated and double-layer coated ZIRLO samples. After longer time (7–26 minutes) in 1000 °C hot steam the lowest hydrogen amount from all the tested samples was released in the case of NCD coated ZIRLO tube.

stress would lead to a degradation of coating in parts close to interface [29,48]. For high protection against metal surface corrosion in hot water environments, different permeable coatings (in terms of mate rials, thicknesses, and technologies) should be selected and used.

### 3.2. Optical microscopy of metallographic cross sections of samples

In the metallographic observation of oxidized coated and standard ZIRLO samples, the inner oxide layer serves as a good reference for oxide layer thickness (Figs. 2 4). Fully protected and unprotected re gions (with the thickest oxide layer) are randomly distributed over the outer surface [29]. As presented in Figs. 2 4, for 2 μm CrAlSiN coated ZIRLO fuel rods treated at 1000 °C for 60 min, the prior β Zr structure is still apparent in fully protected regions. From optical microscopy, it is clear that the CrAlSiN coating serves as a barrier against oxygen dif fusion until mechanical failure of the coating occurs. However, when the CrAlSiN coatings mechanically failed, the oxidation process was even faster than in the case of unprotected samples. After CrAlSiN coated ZIRLO tubes treating at 1000 °C / 60 min (Fig. 2) prior β Zr phase with no oxygen stabilized zirconium alpha phase indicates no, or very low oxygen diffusion through the CrAlSiN coating into the zirco nium metal. Nodular (or “blister”) pattern is quite common on outer surface and indicates places, where protective coating mechanical fails and steam starts to penetrate zirconium alloy through cracks in coating [29].

NCD protects the Zr alloy tube surface homogeneously regardless of cracks and defects in the NCD coating. Figs. 2 4 present metallographic cross sections of NCD coated, CrAlSiN coated and double layer coated ZIRLO tubes treated at 1000 °C/60 min. The thickness of the outer (coated) surface oxide layer varies from the thickness of the (uncoated) inner oxide to different extents for different coatings. The oxidation of the coated part of the tube (outer part) is smallest (compared to the oxidation of the inner part) in the case of the double layer coated ZIRLO tube. In the case of the NCD coated tube, the outer $ZrO_2$ layer thickness is typically 85 90% of the inner oxide layer thickness (corresponding to our previous results published in [27,28]). For the CrAlSiN coating, the outer $ZrO_2$ layer thickness varies from 90 to 95% of the inner oxide layer thickness. For the double layer, the thickness of the outer oxide layer varies from 65 to 75% of the inner oxide layer thickness. These results correspond to the relative weight gains of the coated and au toclaved samples (Figs. 4, S3).

### 3.3. Electron microscopy

Using TEM, we showed that NCD coated zirconium alloy before oxidation was fully covered by the diamond layer. TEM of NCD coated zirconium alloy after oxidation at 400 °C for 4 days indicated that the substrate is only partially covered by the diamond layer after oxidation. Fig. 5 (a) is a cross sectional bright field (BF) TEM image of the NCD on top of a Zr oxide layer. The NCD is indicated by (1), the Zr oxide layer is indicated by (2), and the zirconium alloy is indicated by (3). TEM also confirmed the presence of an amorphous carbon layer between the NCD and the zirconium oxide substrate after oxidation (Fig. 5 (b)).

In our experiments, to determine the impact of CrAlSiN cracking, the thickness of the coating was only 2 μm. Using SEM, we showed that after hot steam oxidation, the number of cracks in the CrAlSiN coating

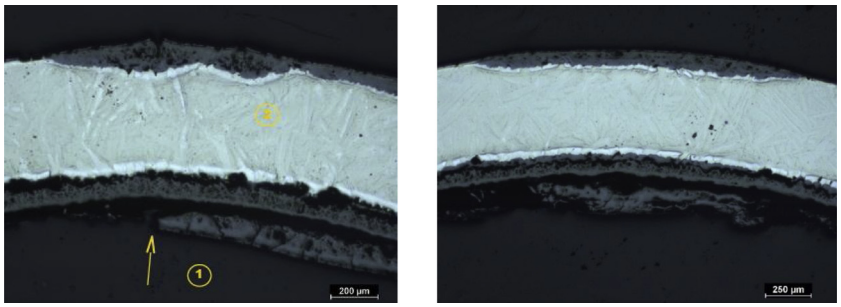


**Fig. 2.** Metallographic observations of CrAlSiN coated ZIRLO tubes treated at 1000 °C / 60 min. Prior β-Zr phase with no oxygen stabilized zirconium alpha phase indicates no, or very low oxygen diffusion through the CrAlSiN coating into the zirconium metal. Nodular (or “blister”) pattern is quite common on outer surface and indicates places, where protective coating mechanical fails and steam starts to penetrate zirconium alloy through cracks in coating [29].

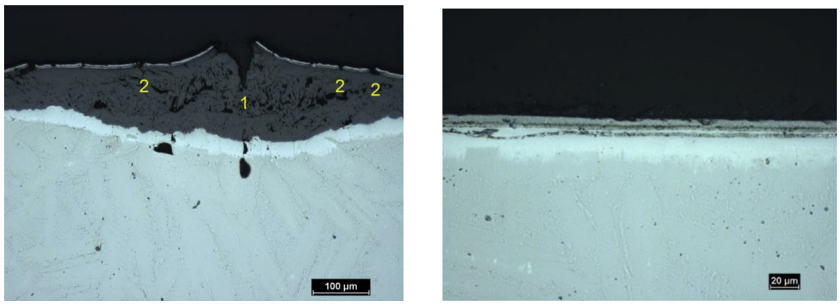


**Fig. 3.** Metallographic observations of CrAlSiN coated ZIRLO tubes treated at 1000 °C / 60 min. Thickness of outer (coated) oxide layer varies from zero to same or even higher thickness than inner oxide. Fully protected and unprotected places (with most thick oxide) are randomly distributed along outer surfaces. Left: Zr oxide "blister", which developed after coating failure with visible initial crack (1) and secondary coating cracks (2). Secondary cracks are caused by expansion of zirconium oxide underneath the coatings. Coating residua are still present on outer surface. Right: Detail of area where no oxidation of zirconium occurred [29].

of the ZIRLO tube grew more rapidly than in the case of hot steam oxidized double layer (CrAlSiN and NCD) coated ZIRLO tubes. After treatment for 4 days at 400 °C under hot steam, the number of cracks in the CrAlSiN coating of double layer coated ZIRLO was smaller than in the case of the hot steam oxidized CrAlSiN coated ZIRLO tube (by 20 30%, according to SEM observation) due to the soft NCD layer ($sp^2$ hybridized C). The underlying NCD layer may mitigate thermal expansion, reducing cracks in the upper layer and defects in CrAlSiN. The SEM of ZIRLO coated with double layers of NCD and CrAlSiN after treatment for 60 min at 1000 °C showed that the number of cracks in the upper CrAlSiN layer increased compared to that in double layer coated ZIRLO tubes treated at 400 °C for 4 days by autoclaving (Fig. 6).

SEM also confirmed that the 500 nm thick NCD coating had the ability to protect ZIRLO nuclear fuel tubes against surface oxidation in autoclaved samples even though cracks and defects were present in the NCD before and after autoclaving (Fig. 7).

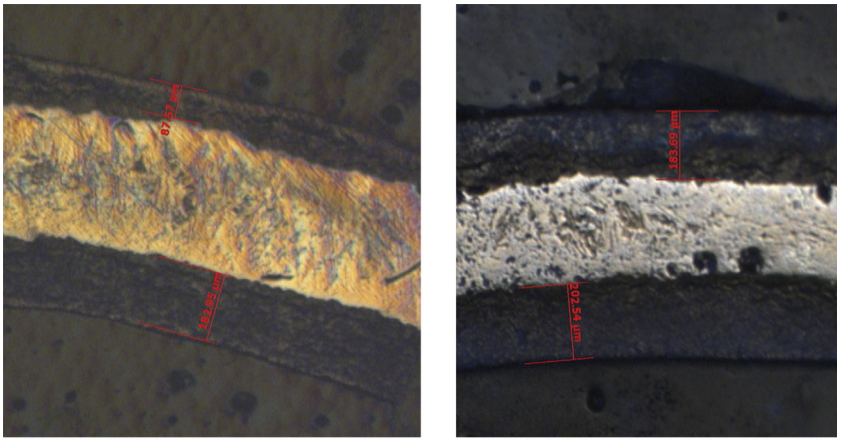


a) b)

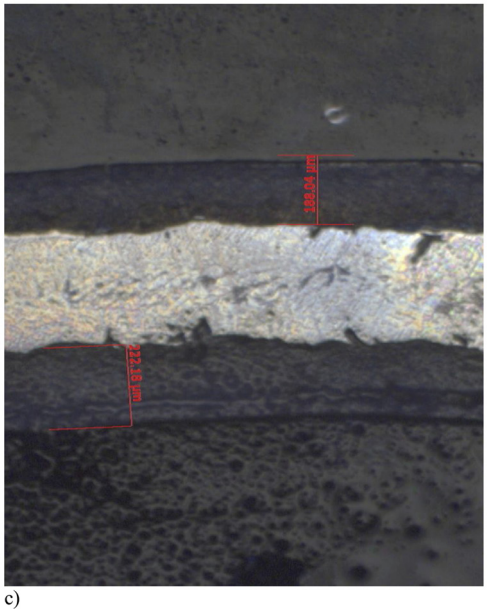


c)

**Fig. 4.** Metallographic observations with marked and stressed thicknesses of oxidized layers: a) CrAlSiN plus NCD double layer-coated ZIRLO tubes treated at 1000 °C/60 min under hot steam. b) CrAlSiN-coated ZIRLO tubes treated at 1000 °C/60 min. under hot steam, c) NCD-coated ZIRLO tubes treated at 1000 °C/60 min. under hot steam.

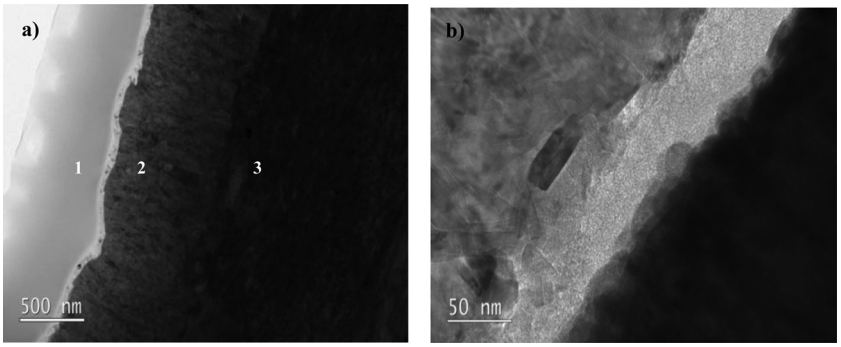


**Fig. 5.** a) BF TEM micrograph of a section cut from an NCD-coated ZIRLO tube showing the (1) diamond layer and (2) Zr oxide layer on top of the (3) Zr alloy. b) BF TEM image showing the presence of an amorphous carbon layer between the NCD and the Zr oxide layer after oxidation.

### *3.4. Secondary ion mass spectrometry*

SIMS is an exceedingly customary method used for observance diffusion and changes of elemental concentration with depth. In Fig. 8 the NCD coating on ZIRLO tube is compared with NCD coated ZIRLO after 1000 °C in hot steam environment. The SIMS data showed that for NCD coated ZIRLO tube after 60 min at a 1000 °C in hot steam en vironment; a peak in carbon content was within the $ZrO_2$ layer 2 μm below the coated sample surface. NCD coating on ZIRLO sample was 0.5 μm thick. In our previous work [27] we have showed that when NCD coated ZIRLO sample was exposed 4 days at 400 °C in autoclave, the carbon diffused from the surface NCD layer so that most of it is located in $ZrO_2$ layer 1.5 μm beneath the sample surface which is in the scope of $ZrO_2$ layer ($ZrO_2$/Zr alloy interface is 2.3 μm under the sample surface) 29].

### *3.5. X ray photoelectron spectroscopy and Raman spectroscopy*

The protective capabilities of the 500 nm NCD layer were illustrated using XPS of NCD coated ZIRLO tubes, double layer coated ZIRLO tubes and standard ZIRLO fuel cladding tubes cut perpendicular to the surface after and before accident and working temperature autoclave tests [6]. XPS of NCD coated ZIRLO sample 4 days autoclaving at 400 °C [27] showed carbides in $ZrO_2$ layer which also change conditions for Zr corrosion.

The NCD coated ZIRLO tubes autoclaved under accident conditions (1000 °C, 60 min) had a surface layer containing a mixture of zirco nium, carbide, carbon and oxidized carbon/graphite (Fig. 9). In these samples, bigger concentration (compared to NCD protected ZIRLO samples not processed by autoclave) of pure carbide and a smaller concentration of oxygen were detected compared to those in the surface layer of the unprotected autoclaved ZIRLO samples. The content of oxygen in autoclaved (1000 °C, 60 min) NCD coated ZIRLO tubes was smaller than that in unprotected autoclaved ZIRLO tubes. (Fig. S4). XPS confirmed that ZIRLO coated with a double layer and treated under accident conditions (1000 °C, 60 min) had oxidized CrAlSiN on the surface and smaller oxidization than uncoated ZIRLO tubes treated under the same conditions. It should be emphasized that XPS is just very thin surface sensitive method. The amount of carbon diffused from NCD coating at 1000 °C is very low it corresponds to density of doping in extrinsic semiconductor. It correlates with the fact that thickness of $ZrO_2$ layer in NCD coated ZIRLO samples after 60 min in 1000 °C hot steam is round 188 μm (Fig. 4) and the 0.5 μm thick NCD layer affect just very thin surface part (2 3 μm) of the whole 188 μm $ZrO_2$ layer and represents 1.4% of the normalized weight gain for the ZIRLO tubes after 1000 °C hot steam, 60 min respectively.

Raman spectra of the ZIRLO tube with a 500 nm NCD film and double layer coated are presented in Suppl. Information (Figs. S5, S6). Individual lines were obtained from different sample sites (labelled in SEM Figs. 6 and 7) and demonstrated the presence of a NCD layer consisting of diamond and graphite phases on the whole surface of the sample. Raman spectra of the ZIRLO tube with a double layer NCD and CrAlSiN coating autoclaved at 400 °C for 4 days [34] are presented in Fig. S6. After autoclave tests, the diamond phase is still present and serves a protective function at sites of disrupted compactness of the CrAlSiN alloy layer.

### *3.6. Capacitance measurements*

#### *3.6.1. Samples oxidized for 4 days at 400 °C in hot steam autoclave*

It has previously been found that the oxide formed on pure ZIRLO tubes exhibits n type semiconductivity [27]. The acceptor ($N_A$) and/or

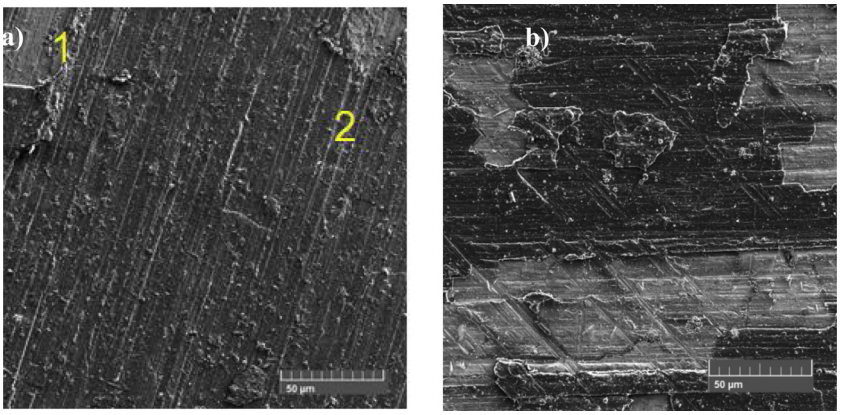


**Fig. 6.** SEM of ZIRLO coated by double layers. a) After 4 days in 400 °C hot steam. b) After 60 min hot steam tests at 1000 °C. The number of cracks in upper CrAlSiN layer strongly raised up. Raman spectra (Fig. S5) were measured at labelled points.

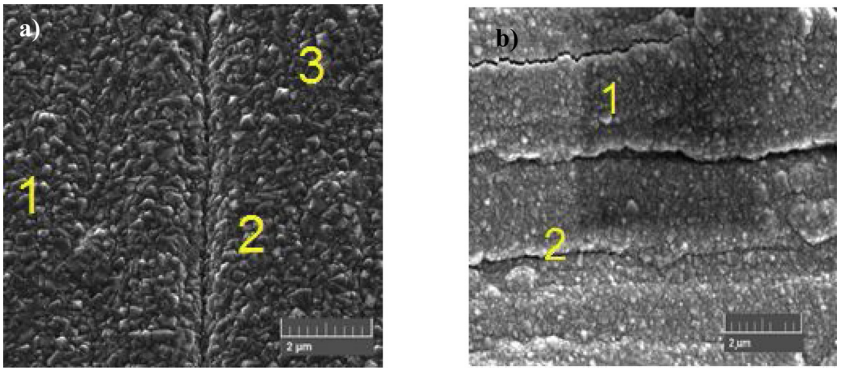


**Fig. 7.** a) SEM of ZIRLO coated by 500 nm NCD, b) SEM of ZIRLO coated by 500 nm NCD after 4 days autoclave tests at 400 °C. At labelled point Raman spectra were collected (Fig S6).

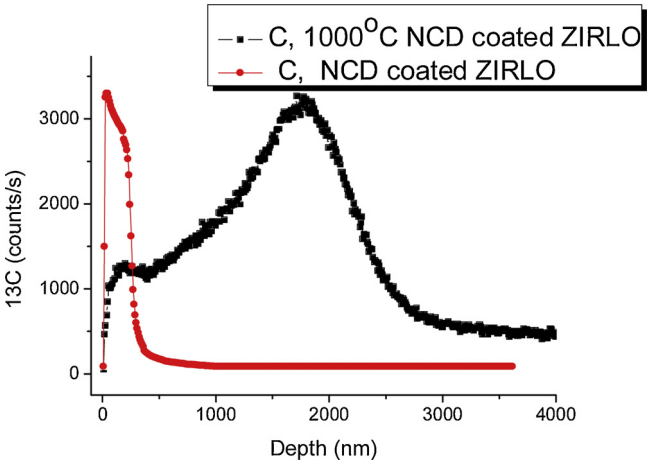


**Fig. 8.** SIMS data from NCD coated ZIRLO tube after 60 min at a 1000 °C in hot steam environment, a peak in carbon content was within the $ZrO_2$ layer 2 µm below the sample surface. NCD coating on ZIRLO sample was 0.5 µm thick.The carbon depth profiles are plotted from the sample surface.

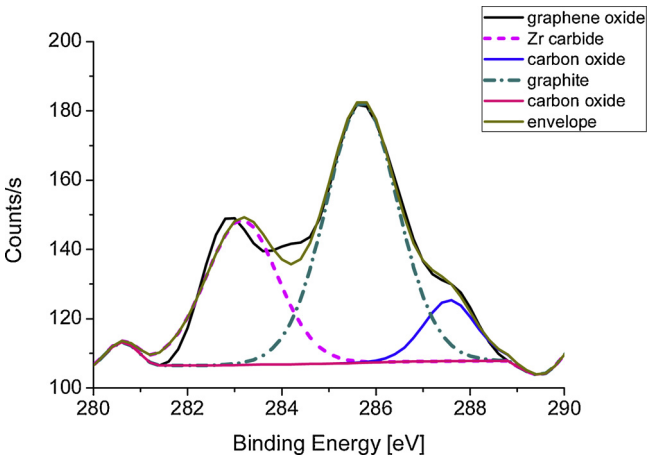


**Fig. 9.** C1s lines of NCD coated ZIRLO after hot steam application 1000 °C, 60 min. Data were calibrated on the Zr 3d5/2 line. The areas analyzed were on the NCD surface. In addition to Zr carbide, different states of oxides are evident: oxidized graphite (285.5 eV), oxidized carbon (287.5 eV), and oxidized carbide (binding energy of 283 eV).

donor ($N_D$) densities are presented in Tab. S1. Uncovered and exposed ZIRLO exhibits n type semiconductivity, while the coated samples ex hibit n and p type semiconductivity.

Through voltage dependent capacitance plots, it was found that pure zirconium oxide is an n type semiconductor. After coating a tube with NCD and exposure to hot steam (4 days at 400 °C), mixed n and p type semiconductor behavior was detected (Tab. S1). Using SIMS in our previous work [1], we showed that after 4 days at 400 °C hot steam in double layer coated ZIRLO cladding the penetration maximum of carbon from the NCD coating into the $ZrO_2$ layer is to a depth of 1 µm. SIMS also showed that the $ZrO_2$ in double layer coated ZIRLO after 60 min of hot steam exposure at 1000 °C contained the majority of the carbon at a 2 µm depth. ZIRLO covered with 2 µm CrAlSiN is an n type semiconductor, and ZIRLO covered with 2 µm CrAlSiN exposed to t 400 °C hot steam autoclave (4 days) is also an n type semiconductor (Tab S1). ZIRLO covered with a double layer and autoclaved for 4 days in 400 °C hot steam has a ZIRLO surface layer ($ZrO_2$) of mixed (n and p type) semiconductivity. This result corresponds with the fact that even in the case of a double layer (NCD and CrAlSiN) coating, the carbon from the NCD layer enters the ZIRLO surface/$ZrO_2$.

We also estimated the electrical field at the interface by assuming that free charge concentration is $n = N_D\ N_A$, where $N_D$ and $N_A$ are taken from Tab. S1. The electrical field at the $ZrO_2$/Zr interface of the ZIRLO coated with CrAlSiN and treated for 4 days at 400 °C is 2.79 times larger than the electrical field at the $ZrO_2$/Zr interface of ZIRLO coated with a double layer and treated for 4 days at 400 °C. The electrical field at the $ZrO_2$/Zr interface of the ZIRLO sample treated for 4 days at 400 °C is 1.75 times larger than the electrical field at the $ZrO_2$/Zr interface of ZIRLO coated with NCD and treated for 4 days at 400 °C.

For the p semiconductor/metal interface, electrons from the metal pass through the interface and occupy positions (holes) in the valence band of semiconductors. In this scenario, O anions passing through the $ZrO_2$ layer were less likely to have originated from water dissociation (compared to n type $ZrO_2$/Zr) lose electrons at the $ZrO_2$/Zr interface, which does not support the process of standard Zr oxidation, as in the case on the n semiconductor/metal interface [26] see Fig. S7.

### *3.6.2. Samples oxidized for 60 min at 1000 °C in hot steam furnace*

Electrochemical impedance spectroscopy measurements were also performed with 3 samples pre exposed for 60 min at 1000 °C: uncoated ZIRLO, ZIRLO coated with 2 µm CrAlSiN and ZIRLO coated with a composite coating of 2 µm CrAlSiN and 0,5 µm NCD. the impedance spectra show a broad capacitive response extended to very high fre quencies. Such a response corresponds to extremely thick oxide layers. Due to the high density of heterogeneities in the oxide layers, the oxide capacitance has a highly dissipative form. Former studies [38,39] have shown that the analysis suggested by Jonscher [49] can be successfully applied in such a case. Assuming that the complex impedance $Z^* = Z' - jZ''$, where $Z'$ is the real and $Z''$ is the imaginary part of im pedance, can be expressed as an electrolyte resistance $R_{el}$ linked in series with a complex capacitance $C^* = C' - jC''$, where $C'$ is the real and $C''$ is the imaginary part of capacitance. The expressions of $C'$ and $C''$ take on the following forms:

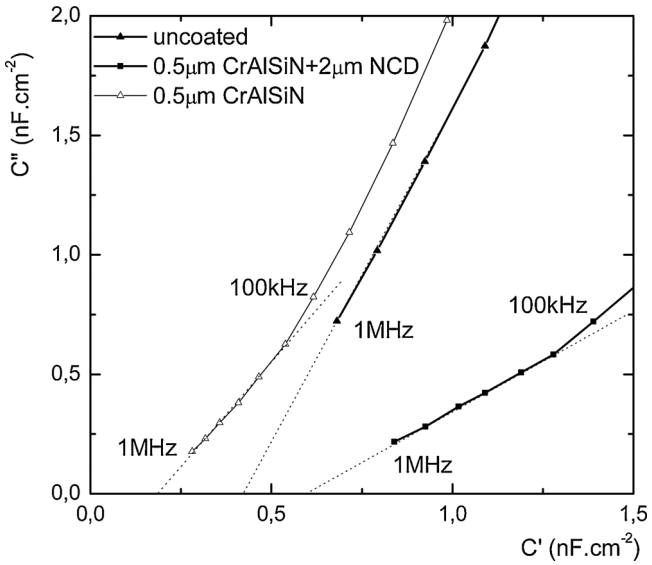


**Fig. 10.** Complex capacitance plot for frequencies of 100 kHz to 1 MHz. Measured in 0,5 M $K_2SO_4$; samples were pre-exposed in steam at 1000 °C for 60 min.

$$C' = \frac{1}{\omega}\frac{Z''}{(Z' - R_{el})^2 + Z''^2} \qquad (2)$$

$$C'' = \frac{1}{\omega}\frac{Z' - R_{el}}{(Z' - R_{el})^2 + Z''^2}$$

where $R_{el}$ is the electrolyte resistance. The Cole Cole diagram expresses the relation between the imaginary and the real part of capacitance. An example of a high frequency region of the complex capacitance data measured for samples pre exposed to 1000 °C hot steam is presented in Fig. 10.

The linear portions of the plots in Fig. 10 correspond to the universal law of dielectric response proposed by Jonscher [49]:

$$C^* = C_{inf} + \frac{B^*}{(j\omega)^{1-n}} \qquad (3)$$

where $B^*$ is a constant related to the dielectric dispersion and $n$ is the dispersion index, characteristic of the constant phase angle between the real axis and the experimental curve. $C_{inf}$ is the capacitance at infinite frequency and can be obtained from the high frequency intercept of the linear extrapolation of the experimental curve to the real axis in the complex capacitance plane.

Oxide thickness is usually calculated using the expression for a flat capacitor:

$$\delta = \frac{A\varepsilon_r\varepsilon_o}{C_{inf}} \qquad (4)$$

where $\varepsilon_o$ is vacuum permittivity ($8.854 \times 10^{-14}$ F. cm $^1$), $\varepsilon_r$ is the relative permittivity of the oxide layer ($\Sigma_r = 23$ for $ZrO_2$) and $A$ is the area of the working electrode. For a relative permittivity of 23, no reasonable results corresponding to the metallographic observations can be obtained from Eq. (2). This is due to the intensive penetration of water into cracks and pores and the resulting increase in the relative permittivity of the oxide layer. By using the approximate oxide thickness from metallographic observations, the effective dielectric constant can be calculated:

$$\varepsilon_{r(eff)} = \frac{\delta C_{inf}}{\varepsilon_o A} \qquad (5)$$

Tab. S2 summarizes the estimated capacitance and effective dielectric constant values. Evidently, the highest content of water in cracks and pores of the oxide was found in the case of uncoated ZIRLO. The coated samples have lower water contents and therefore generally lower porosity. Thicknesses of $ZrO_2$ layers on surface of 60 min, 1000 °C steam treated samples correspond to results obtained from optical microscopy (Fig. 4).

## 4. Conclusions

In this work, a new strategy for protecting metal surfaces against degradation caused by high temperature oxidation is presented. We were the first to prepare a double layered coating consisting of an active and passive part as a protective element for Zr alloy surface against high temperature oxidation in a hot water environment. ZIRLO nuclear fuel cladding was protected against oxidation in water cooled nuclear reactors by coating with a double layer consisting of an active 500 nm thin NCD layer (bottom) and a passive 2 μm thin CrAlSiN (upper) layer.

Double layer coatings reduce ZIRLO nuclear fuel tube oxidation by more than 88% compared to that of uncoated ZIRLO tubes treated for 4 days in 400 °C hot steam. The 2 μm CrAlSiN coating has a similar ability to protect ZIRLO tubes against oxidation after 4 days in 400 °C hot steam. Such a high protective ability of both types of coating (double layer and CrAlSiN) means that during treatment for 4 days at 400 °C in the autoclave, the CrAlSiN coating is destroyed to a relatively small extent and acts as an impermeable barrier. This result also confirms good adhesion of CrAlSiN coating both to ZIRLO surface and to NCD coated ZIRLO surface.

To describe the specific oxidation process of double layer coated ZIRLO coated samples at accident temperature, we tested the critical oxidation kinetics of coated and standard ZIRLO samples treated for 60 min at 1000 °C in a hot steam furnace. At the initial oxidation stage (< 10 min) in the 1000 °C hot steam furnace, CrAlSiN acted as a barrier against surface oxidation. The corrosion of bare ZIRLO and NCD coated ZIRLO was similar as carbon diffusion from NCD coating just begins and does not significantly affect oxidation kinetics of zirconium alloy. On the contrary, CrAlSiN and double layer coating at this initial stage importantly affect the typical oxidation kinetics of zirconium mainly due to small amount of defects in CrAlSiN coating However, for longer oxidation times (> 10 min) in the 1000 °C hot steam furnace the oxidation of CrAlSiN coated ZIRLO was higher than the oxidation of ZIRLO coated with a double layer as the CrAlSiN coating was typically more cracked [29],. At this stage carbon from NCD coating diffuse into growing $ZrO_2$ layer and by changing its electrical properties decrease ZIRLO corrosion. This process of CrAlSiN and double layer coated surface oxidation in the 1000 °C hot steam furnace was confirmed by hydrogen release measurements.

Metallographic observations of ZIRLO samples treated in 1000 °C steam for 60 min showed that the double layer coated part of the ZIRLO tubes had oxide layer thicknesses from 65 to 75% of the thickness of the uncoated ZIRLO oxide layer treated under the same conditions. These results correspond with the measured oxidation of coated and bare ZIRLO samples treated at a 1000 °C in steam furnace for 60 min (capacitance). Moreover, as shown by SEM of double layer coated ZIRLO, the number of cracks in the CrAlSiN coating was smaller than that in the case of autoclaved CrAlSiN coated ZIRLO tubes (by 20 30%, according to SEM observation). If a thicker CrAlSiN coating is applied to NCD covered ZIRLO nuclear fuel claddings, the complex double coating protection ability will be further improved. Double layer coated ZIRLO samples and CrAlSiN coated ZIRLO samples treated at 1000 °C for 60 min had lower porosity of the oxidized surface portion than the uncoated samples under the same treatment (measured by capacitance/Mott Schottky method).

NCD coating consisting of $sp^3$ and $sp^2$ carbon phases with a high crystalline diamond content (96%) reduces Zr nuclear fuel cladding oxidation compared to that of uncoated ZIRLO samples with the same treatment: at operating temperatures, oxidation was typically reduced by 40%; under treatment at 1000 °C for 30 min, oxidation was typically reduced by 17 20%, and hydrogen uptake into the Zr alloy was also

reduced. The NCD coating has the ability to protect Zr alloy nuclear fuel tubes against surface oxidation even when the NCD coating is cracked, as shown by SEM of coated samples oxidized in hot steam. The active protection of NCD coatings is based on the fact that during hot steam or hot water processing, carbon penetrates into $ZrO_2$ (confirmed by XPS, SEM and SIMS). SIMS showed that after 60 min at 1000 °C in hot steam, a peak in carbon content was observed in the $ZrO_2$ layer formed 2 μm beneath the sample surface. In [27] we showed that most of carbon diffused from the surface NCD layer is located in $ZrO_2$ layer 1.5 μm beneath the sample surface which is in the scope of $ZrO_2$ layer ($ZrO_2$/Zr alloy interface is 2.3 μm under the sample surface) [29]. Incorporation of carbon into the $ZrO_2$ layer changes the semiconductivity of the $ZrO_2$ surface from n type to mixed n and p type, consequently changing the electric field at the $ZrO_2$/Zr interface, which represents important obstacle for Zr oxidation at the $ZrO_2$/Zr interface (measured by the capacitance/Mott Schottky method) [27,50].

The CrAlSiN coating is a homogeneous one phase layer. From optical microscopy and SEM, it is clear that the CrAlSiN coating serves as a full barrier against oxygen diffusion until mechanical failure of the coating occurs. When the CrAlSiN coatings mechanically failed [29], the oxidation process was even faster than in the case of unprotected samples. CrAlSiN coating cracking was larger for samples processed at 1000 °C for 60 min than samples processed at 400 °C for 4 days (SEM). For double layers, coating the underlying NCD layer mitigates thermal expansion, reducing cracks in the upper layer and decreasing the defects in CrAlSiN (SEM).

In summary, we created a double layer coating with combined functional properties (active and passive) to protect Zr alloy surface against high temperature oxidation in a water environment. The aim of this work was to show the principle of the double layer coating anticorrosion function. In our case, the bottom NCD water permeable coating served as the active antioxidation element. During high temperature treatment, carbon incorporation into Zr alloy nuclear fuel cladding tubes changed the physical, chemical and structural properties, which worsened the conditions for the Zr alloy oxidation process. The water impermeable top CrAlSiN coating passively prevents physical contact of the Zr cladding tube surface with hot steam. To determine the impact of the CrAlSiN coating in the double layer, the thickness of the CrAlSiN layer was relatively thin only 2 μm. Usually, when a metal surface is protected against hot steam/water oxidation by a water impermeable coating [9,12,16,29], layers on the order of tens of μm in thickness are used.

The demonstrated Zr alloy surface protection against high temperature corrosion obtained by coating a double layered structure with active and passive functional properties is a new principle. Importantly, the double layer coating combines both advantages in hot steam: initially, the top impermeable layer acts as a barrier against water molecules, and after a longer time in hot steam, the water permeable coating NCD effectively worsens the conditions for protecting metal oxidation. The demonstrated strategies can generally be used to protect different metal materials against high temperature corrosion in water environments. To obtain a higher antioxidation function, an impermeable coating made with the different materials, thickness and technologies should be used.

## Data availability

All the data are presented as tables or graphs in the manuscript. Data can be obtained from graphs/Figs (Figs. 1, S1, 9) using Origin software.

## Declaration of Competing Interest

There are no conflicts to declare.

## Acknowledgments

This research was partially supported by the Grant Agency of Czech Technical University in Prague (No. SGS16/244/OHK4/3T/14) and Technological Agency of the Czech RepublicTK02030069. The South African authors acknowledge the National Research Foundation for financial support. This work was supported in part by the MEYS SAFMAT CZ.02.1.01/0.0/0.0/16 013/0001406, LO1409 and LM2015088 projects (SEM maintenance) European Structural and Investment Funds and the Czech Ministry of Education, Youth and Sports SOLID21 CZ.02.1.01/0.0/0.0/16 019/0000760LQ1603 (Research for SUSEN) of the Ministry of Education, Youth and Sports of the Czech Republic and LTC17083 in frame of the COST CA15107.

## Appendix A. Supplementary data

Supplementary material related to this article can be found, in the online version, at doi:https://doi.org/10.1016/j.corsci.2019.108270.

## References

[1] P. Barberis, T. MerleMejean, P. Quintard, On Raman spectroscopy of zirconium oxide films, J. Nucl. Mater. 246 (1997) 232–243.
[2] J. Godlewski, J.P. Gros, M. Lambertin, J.F. Wadier, H. Weidinger, Raman-Spectroscopy Study of the Tetragonal-To-Monoclinic Transition in Zirconium-Oxide Scales and Determination of Overall Oxygen Diffusion by Nuclear Microanalysis of O-18, (1991).
[3] L. Kurpaska, J. Favergeon, L. Lahoche, M. El-Marssi, J.L.G. Poussard, G. Moulin, J.M. Roelandt, Raman spectroscopy analysis of air grown oxide scale developed on pure zirconium substrate, J. Nucl. Mater. 466 (2015) 460–467.
[4] L. Kurpaska, J. Favergeon, J.L. Grosseau-Poussard, L. Lahoche, G. Moulin, In-situ stress analysis of the Zr/ZrO2 system as studied by Raman spectroscopy and deflection test in monofacial oxidation techniques, Appl. Surf. Sci. 385 (2016) 106–112.
[5] L. Kurpaska, M. Frelek-Kozak, J.L. Grosseau-Poussard, I. Jozwik, L. Lahoche, J. Favergeon, J. Jagielski, Identification of the zirconia phases by means of raman spectroscopy for specimens prepared by FIB lift-out technique, Oxid. Met. 88 (2017) 521–530.
[6] P. Meisterjahn, H.W. Hoppe, J.W. Schultze, Electrochemical and XPS measurements on Thin Oxide-Films on Zirconium, J. Electroanal. Chem. 217 (1987) 159–185.
[7] A. Couet, A.T. Motta, A. Ambard, The coupled current charge compensation model for zirconium alloy fuel cladding oxidation: I. Parabolic oxidation of zirconium alloys, Corrosion Sci. 100 (2015) 73–84.
[8] K.I. Choudhry, S. Mahboubi, G.A. Botton, J.R. Kish, I.M. Svishchev, Corrosion of engineering materials in a supercritical water cooled reactor: characterization of oxide scales on Alloy 800H and stainless steel 316, Corrosion Sci. 100 (2015) 222–230.
[9] U. Wiklund, P. Hedenqvist, S. Hogmark, B. Stridh, M. Arbell, Multilayer coatings as corrosion protection of Zircaloy, Surf. Coat. Technol. 86-7 (1996) 530–534.
[10] B. Cox, Some thoughts on the mechanisms of in-reactor corrosion of zirconium alloys, J. Nucl. Mater. 336 (2005) 331–368.
[11] G. Saji, Root cause study on hydrogen generation and explosion through radiation-induced electrolysis in the Fukushima Daiichi accident, Nucl. Eng. Des. 307 (2016) 64–76.
[12] D.L. Jin, F. Yang, Z.H. Zou, L.J. Gu, X.F. Zhao, F.W. Guo, P. Xiao, A study of the zirconium alloy protection by Cr3C2-NiCr coating for nuclear reactor application, Surf. Coat. Technol. 287 (2016) 55–60.
[13] A.E. Karkin, V.I. Voronin, I.F. Berger, V.A. Kazantsev, Y.S. Ponosov, V.G. Ralchenko, V.I. Konov, B.N. Goshchitskii, Neutron irradiation effects in chemical-vapor-deposited diamond, Phys. Rev. B 78 (2008).
[14] C. Tang, M. Stueber, H.J. Seifert, M. Steinbrueck, Protective coatings on zirconium-based alloys as accident-tolerant fuel (ATF) claddings, Corros. Rev. 35 (2017) 141–165.
[15] Y.Z. Chen, M. Urquidi-Macdonald, D.D. Macdonald, The electrochemistry of zirconium in aqueous solutions at elevated temperatures and pressures, J. Nucl. Mater. 348 (2006) 133–147.
[16] W.C. Zhong, P.A. Mouche, X.C. Han, B.J. Heuser, K.K. Mandapaka, G.S. Was, Performance of iron-chromium-aluminum alloy surface coatings on Zircaloy 2 under high-temperature steam and normal BWR operating conditions, J. Nucl. Mater. 470 (2016) 327–338.
[17] V.A. Avincola, M. Grosse, U. Stegmaier, M. Steinbrueck, H.J. Seifert, Oxidation at high temperatures in steam atmosphere and quench of silicon carbide composites for nuclear application, Nucl. Eng. Des. 295 (2015) 468–478.
[18] D.J. Young, High Temperature Oxidation and Corrosion of Metals, 2nd edition, Elsevier Science Ltd, Oxford, 2016.
[19] E.N. Hoffman, D.W. Vinson, R.L. Sindelar, D.J. Tallman, G. Kohse, M.W. Barsoum, MAX phase carbides and nitrides: properties for future nuclear power plant in-core applications and neutron transmutation analysis, Nucl. Eng. Des. 244 (2012) 17–24.
[20] A.T. Motta, A. Couet, R.J. Comstock, Corrosion of zirconium alloys used for nuclear

fuel cladding, in: D.R. Clarke (Ed.), Annual Review of Materials Research, Vol 45 2015, pp. 311–343.
[21] N. Ni, S. Lozano-Perez, J.M. Sykes, G.D.W. Smith, C.R.M. Grovenor, Focussed ion beam sectioning for the 3D characterisation of cracking in oxide scales formed on commercial ZIRLO (TM) alloys during corrosion in high temperature pressurised water, Corrosion Sci. 53 (2011) 4073–4083.
[22] L.Y. Chen, J.X. Li, Y. Zhang, L.C. Zhang, W.J. Lu, L.Q. Wang, L.F. Zhang, D. Zhang, Zr-Sn-Nb-Fe-Si-O alloy for fuel cladding candidate: processing, microstructure, corrosion resistance and tensile behavior, Corrosion Sci. 100 (2015) 332–340.
[23] B.D.C. Bell, S.T. Murphy, P.A. Burr, R.J. Comstock, J.M. Partezana, R.W. Grimes, M.R. Wenman, The influence of alloying elements on the corrosion of Zr alloys, Corrosion Sci. 105 (2016) 36–43.
[24] G.H. Yuan, G.Q. Cao, Q. Yue, L. Yang, Y.F. Yun, G.S. Shao, J.H. Hu, Formation and fine-structures of nano-precipitates in ZIRLO, J. Alloys. Compd. 687 (2016) 451–457.
[25] D. Khatamian, Solubility and partitioning of hydrogen in metastable Zr-based alloys used in the nuclear industry, J. Alloys. Compd. 293 (1999) 893–899.
[26] V.V. E.I.A. Likhanskii, Review of theoretical conceptions on regimes of oxidation and hydrogen pickup in Zr-alloys, Nuclear Fuel Cycle Fuel Mater. 17 (S11) (2008) 1–17.
[27] J. Skarohlid, P. Ashcheulov, R. Skoda, A. Taylor, R. Ctvrtlik, J. Tomastik, F. Fendrych, J. Kopecek, V. Chab, S. Cichon, P. Sajdl, J. Macak, P. Xu, J.M. Partezana, J. Lorincik, J. Prehradna, M. Steinbruck, I. Kratochvilova, Nanocrystalline diamond protects Zr cladding surface against oxygen and hydrogen uptake: nuclear fuel durability enhancement, Sci. Rep. 7 (2017) 14.
[28] P. Ashcheulov, R. Skoda, J. Skarohlid, A. Taylor, L. Fekete, F. Fendrych, R. Vega, L. Shao, L. Kalvoda, S. Vratislav, V. Chab, K. Horakova, K. Kusova, L. Klimsa, J. Kopecek, P. Sajdl, J. Macak, S. Johnson, I. Kratochvilova, Thin polycrystalline diamond films protecting zirconium alloys surfaces: From technology to layer analysis and application in nuclear facilities, Appl. Surf. Sci. 359 (2015) 621–628.
[29] J.Š. Škarohlíd, High temperature behaviour of CrAlSiN MAX phase coatings on zirconium alloy, R, Water Reactor Fuel Performance Meeting, Jeju Island, South Corea, 2017.
[30] I. Kratochvilova, R. Skoda, J. Skarohlid, P. Ashcheulov, A. Jager, J. Racek, A. Taylor, L. Shao, Nanosized polycrystalline diamond cladding for surface protection of zirconium nuclear fuel tubes, J. Mater. Process. Technol. 214 (2014) 2600–2605.
[31] R. Škoda, Škarohlíd, J., Kratochvílová, I., Taylor, A., Fendrych, Layer protecting the surface of zirconium alloys used in nuclear reactors., in: I.o.P.A.C. Czech Technical University in Prague Faculty of Mechanical Engineering (Ed.) Czech patent 305059 (2015), Czech Republic, 2015.
[32] F. Fendrych, A. Taylor, L. Peksa, I. Kratochvilova, J. Vlcek, V. Rezacova, V. Petrak, Z. Kluiber, L. Fekete, M. Liehr, M. Nesladek, Growth and characterization of nanodiamond layers prepared using the plasma-enhanced linear antennas microwave CVD system, Journal of Physics D-Applied Physics 43 (2010).
[33] P. Ashcheulov, A. Taylor, V. Mortet, A. Poruba, F. Le Formal, H. Krysova, M. Klementova, P. Hubik, J. Kopecek, J. Lorincik, J.-H. Yum, I. Kratochvilova, L. Kavan, K. Sivula, Nanocrystalline boron-doped diamond as a corrosion-resistant anode for water oxidation via Si Photoelectrodes, ACS Appl. Mater. Interfaces 10 (2018) 29552–29564.
[34] K. Lukaszkowicz, J. Sondor, K. Balin, J. Kubacki, Characteristics of CrAlSiN plus DLC coating deposited by lateral rotating cathode arc PVD and PACVD process, Appl. Surf. Sci. 312 (2014) 126–133.
[35] I. Kratochvilova, J. Sebera, P. Ashcheulov, M. Golan, M. Ledvina, J. Micova, F. Mravec, A. Kovalenko, D. Zverev, B. Yavkin, S. Orlinskii, S. Zalis, A. Fiserova, J. Richter, L. Sefc, J. Turanek, Magnetical and optical properties of nanodiamonds can Be tuned by particles surface chemistry: theoretical and experimental study, J. Phys. Chem. C 118 (2014) 25245–25252.
[36] Standard Test Method for Corrosion Testing of Products of Zirconium, Hafnium, and Their Alloys in Water at 680°f (360°C) or in Steam at 750°f (400°C), ASTM G2 / G2M-06 (2011) e1 in, (2011) (201), https://www.astm.org/Standards/G2.htm.
[37] R. Skoda, J. Skarohlid, I. Kratochvilova, F. Fendrych, A.J. Taylor, Layer for protecting surface of zirconium alloys in e.g. PWR, has homogenous polycrystalline diamond layer prepared by chemical vapor deposition process, where thickness of polycrystalline diamond later is provided from specific range, Univ Czech Tech Prague Faculty Electr; Acad Sci Czech Republic Inst Physics; Ceske Vysoke Uceni Tech Praze Fakulta; Ceske Vysoke Uceni Tech V Praze Fakulta; Fyzikalni Ustav Avcr Vvi; Inst Physics Acad Sci Czech Republic; Univ Czech Tech in Prague Faculty Electr.
[38] J. Macak, P. Sajdl, P. Kucera, R. Novotny, J. Vosta, In situ electrochemical impedance and noise measurements of corroding stainless steel in high temperature water, Electrochim. Acta 51 (2006) 3566–3577.
[39] A. Krausova, J. Macak, P. Sajdl, R. Novotny, V. Renciukova, V. Vrtilkova, In-situ electrochemical study of Zr1nb alloy corrosion in high temperature Li+ containing water, J. Nucl. Phys. Mater. Sci. Radiat. Appl. 467 (2015) 302–310.
[40] C.C. Tang, M. Stueber, H.J. Seifert, M. Steinbrueck, Protective coatings on zirconium-based alloys as accident-tolerant fuel (ATF) claddings, Corros. Rev. 35 (2017) 141–165.
[41] X.F. Ma, Y.W. Wu, J. Tan, C.Y. Meng, L. Yang, W.A. Dang, X.J. He, Evaluation of corrosion and oxidation behaviors of TiAlCrN coatings for nuclear fuel cladding, Surf. Coat. Technol. 358 (2019) 521–530.
[42] E. Alat, A.T. Motta, R.J. Comstock, J.M. Partezana, D.E. Wolfe, Ceramic coating for corrosion (c3) resistance of nuclear fuel cladding, Surf. Coat. Technol. 281 (2015) 133–143.
[43] Y. Kurata, M. Futakawa, Corrosion of CrN-coated steels for nuclear reactors in liquid Pb-Bi, J. Jpn. Inst. Met. 72 (2008) 470–476.
[44] T.G. Wei, R.Q. Zhang, H.Y. Yang, H. Liu, S.Y. Qiu, Y. Wang, P.N. Du, K. He, X.G. Hu, C. Dong, Microstructure, corrosion resistance and oxidation behavior of Cr-coatings on Zircaloy-4 prepared by vacuum arc plasma deposition, Corrosion Sci. 158 (2019) 12.
[45] Z. Yang, X.F. Fan, C.J. Qiu, X. Yang, Y.H. Liu, X.J. Wang, High temperature and high pressure flowing water corrosion resistance of multi-arc ion plating Cr/TiAlN and Cr/TiAlSiN coatings, Mater. Res. Express 6 (2019) 10.
[46] V. Chakarova, T. Boiadjieva-Scherzer, D. Kovacheva, H. Kronberger, M. Monev, Corrosion behaviour of electrodeposited Zn-Cr alloy coatings, Corrosion Sci. 140 (2018) 73–78.
[47] X.C. Zhang, B.S. Xu, H.D. Wang, Y. Jiang, Y.X. Wu, Prediction of three-dimensional residual stresses in the multilayer coating-based systems with cylindrical geometry, Compos. Sci. Technol. 66 (2006) 2249–2256.
[48] X.C. Zhang, B.S. Xu, H.D. Wang, Y.X. Wu, Effect of graded interlayer on the mode I edge delamination by residual stresses in multilayer coating-based systems, Appl. Surf. Sci. 254 (2008) 1881–1889.
[49] A.K. Jonscher, A new understanding of the Dielectric-Relaxation of Solids, J. Mater. Sci. 16 (1981) 2037–2060.
[50] Irena Kratochvílová, Andrew Taylor, Jan Škarohlíd, Petr Ashcheulov, František Fendrych, Advanced Coating Materials Chapter : Polycrystalline Diamond Coating Protects Zr Cladding Surface Against Corrosion in Water-cooled Nuclear Reactors: Nuclear Fuel Durability Enhancement, WILEY-Scrivener, USA, 2018.